

# Sonochemical Preparation of Single-Dispersion Metal Nanoparticles from Metal Salts

Toshiyuki Fujimoto,<sup>\*,†</sup> Shin-ya Terauchi,<sup>†</sup> Hiroyuki Umehara,<sup>†</sup> Isao Kojima,<sup>†</sup> and William Henderson<sup>‡</sup>

National Institute of Materials and Chemical Research, Tsukuba, Japan

Received November 15, 2000. Revised Manuscript Received January 17, 2001

Novel metal nanoparticles of Pd and Pt were prepared by sonochemical reduction of solutions containing H<sub>2</sub>PtCl<sub>6</sub> or K<sub>2</sub>PdCl<sub>4</sub>. The effect of atmospheric gas on the particle size distribution was investigated. Average diameters and standard deviations of the Pd particles prepared under Ar (Pd/Ar) and N<sub>2</sub> (Pd/N<sub>2</sub>) were found to be 3.6 ± 0.7 nm (Pd/Ar) and 2.0 ± 0.3 nm (Pd/N<sub>2</sub>). Smaller and sharper distribution of the particle size was observed for the Pd particles formed under a N<sub>2</sub> atmosphere. In the case of Pt, a smaller and sharper distribution of the particle size was observed for the particles prepared under a Xe atmosphere. These relations can be explained in terms of a hot-spot temperature created by acoustic cavitation.

## 1. Introduction

Novel metal nanoparticles have been used in many fields such as catalysis and optics. They also have potential applications in quantum electronic devices. To design high-performance materials, it is of paramount importance that particle sizes and structures be controlled.

On the other hand, ultrasound has become an important tool in chemistry. When solutions are exposed to strong ultrasound, bubbles in solution are implodingly collapsed by acoustic fields, and high-temperature and high-pressure fields are produced at the centers of the bubbles. This effect is known as acoustic cavitation. The temperature of the hot spot has been estimated to be over 5000 K, which is high enough to decompose molecules in bubbles.<sup>1</sup> Suslick et al. have applied this phenomenon to prepare amorphous iron from Fe(CO)<sub>5</sub>.<sup>2</sup> The formation of Ag and Au nanoparticles using ultrasonic irradiation of aqueous solutions has been reported.<sup>3,4</sup> Recently, the formation of Au/Pd and Pt/Pd bimetallic particles were also reported.<sup>5,6</sup>

Ultrasound offers a very attractive method for the synthesis of metal nanoparticles, and the advantages of this method include a rapid reaction rate and the ability to form very small metal particles. However, metal nanoparticles prepared by sonochemical reduction

generally have wider size distributions. Some efforts to control the particle size and size distribution using different initial metal concentrations,<sup>7,8</sup> surfactant types, and coexisting alcohol types<sup>4,8</sup> have been reported. Because the temperature generated in the localized hot spot depends on the properties (heat capacity and thermal conductivity) of the gases inside the bubble,<sup>9</sup> the difference of the atmospheric gas might provide different reaction conditions. Here, we report the effect of the atmospheric gas on the particle size and size distribution of nanoparticles prepared using ultrasonic irradiation.

## 2. Experimental Section

Metal salts (H<sub>2</sub>PtCl<sub>6</sub>·6H<sub>2</sub>O, K<sub>2</sub>PdCl<sub>4</sub>) were dissolved in gas-saturated (N<sub>2</sub>, Ar, or Xe) water to make 1 mmol dm<sup>-3</sup> solutions, and poly(*N*-vinyl-2-pyrrolidone) (PVP, K-30, MW = 40 000) was added as a protecting agent. The concentration of PVP was ca. 0.1 mmol of monomeric unit dm<sup>-3</sup>. The metal salt solutions (19 mL) and 1 mL of gas-saturated 2-propanol were placed into the cylindrical sonication reactor (glass made, 25 mm diameter), which was placed in a water bath. Because the local heating produced by the cavitation also depends on the solution temperature,<sup>10</sup> the temperature of the water bath was held at 278 ± 0.5 K during sonication.

Ultrasonic irradiation was performed with a collimated 20-kHz beam from a ceramic transducer with a titanium amplifying horn (Sonics and Materials, VCX-600) directly immersed in the solution. The power of the ultrasound was 100 W. The sonication reactor and titanium horn were connected by an O-ring. A schematic of the reactor is represented in Figure 1. Because the reactor has a Teflon valve, the solutions can be treated without exposure to air by standard Schlenk techniques. The irradiation was stopped at various times, and UV-vis spectra were recorded using a UV-Vis2000 (Shimadzu)

\* Author to whom correspondence should be addressed. Tel.: +81 298 614 627. Fax: +81 298 614 627. E-mail: fuji@nimc.go.jp.

<sup>†</sup> National Institute of Materials and Chemical Research.

<sup>‡</sup> On leave from the University of Waikato, Hamilton, New Zealand.

(1) Flint, E. B.; Suslick, K. *Science* **1991**, *253*, 1397.

(2) Suslick, K.; Choe, S.-B.; Cichowlas, A. A.; Grinstaff, M. W. *Nature* **1991**, *353*, 414.

(3) Nagata, Y.; Watanabe, Y.; Fujita, S.; Dohmaru, T.; Taniguchi, S. *Chem. Commun.* **1992**, 1620.

(4) Yeung, S. A.; Hobson, R.; Biggs, S.; Grieser, F. *Chem. Commun.* **1993**, 378.

(5) Mizukoshi, Y.; Okitsu, K.; Maeda, Y.; Yamamoto, T.; Oshima, R.; Nagata, Y. *J. Phys. Chem. B* **1997**, *101*, 7033.

(6) Fujimoto, T.; Terauchi, S.; Umehara, H.; Kojima, I.; Henderson, W. *Mater. Res. Soc. Symp. Proc.* **1998**, *497*, 129.

(7) Cao, X.; Koltypin, Y.; Kataby, G.; Prozorov, R.; Gedanken, A. *J. Mater. Res.* **1995**, *10*, 2952.

(8) Okitsu, K.; Bandow, H.; Maeda, Y.; Nagata, Y. *Chem. Mater.* **1996**, *8*, 315.

(9) Flint, E. B.; Suslick, K. *J. Am. Chem. Soc.* **1989**, *111*, 6987.

(10) Hiller, R.; Putterman, S. J.; Barber, B. P. *Phys. Rev. Lett.* **1992**, *69*, 1182.

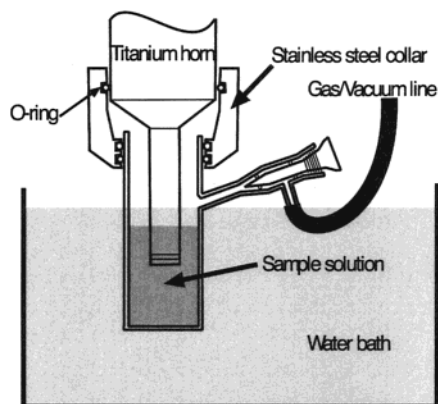


**Figure 1.** Schematics of the sonication reactor.

instrument. Some drops of the solutions were placed onto a carbon support film stuck on a copper microgrid and vacuum-dried.

Transmission electron microscopy was performed using a JEOL2000FXII instrument. The sizes of 500 particles were measured on micrographs in order to obtain average diameters and size distributions. All manipulations were performed under appropriate gas atmosphere except when the microgrids were introduced into the electron microscope.

### 3. Results

**3.1. Palladium Nanoparticles.** In the case of a Pd salt aqueous solution under an Ar atmosphere, the initial clear yellow-orange solution changed to a very pale color and then turned dark brown upon ultrasonic irradiation. In the UV-vis spectrum, absorption bands at around 425 and 310 nm, which were characteristic before sonication, first decayed with an increase of the baseline observed during the sonication. Characteristic absorptions were almost completely diminished after 7 min of sonication. (This is denoted as the first stage.) The solution color became darker upon further sonication, and the point at which no further change in the UV-vis spectra was observed was chosen as the reaction finish (18 min). Electron microscopy revealed that the average diameter ( $D_{AVE}$ ) and the standard deviation of the particle size ( $D_{STD}$ ) are 3.6 and 0.7 nm, respectively. Although edges are observed for some particles, most are spherical.

A Xe-saturated aqueous solution showed a similar sequence during sonication; however, the reaction proceeded much more rapidly. The first stage of the reaction was finished within 1 min, and the reaction was completed after 4 min. For the final solution, the increase of the UV-vis baseline was greater than that under an Ar atmosphere, indicating the formation of larger particles. Indeed,  $D_{AVE}$  and  $D_{STD}$  were estimated to be 4.1 and 5.1 nm, respectively, by electron microscopy. The particles were very irregular in size. Overall, the particle sizes were distributed in the range of 1.1–40.6 nm, although more than 65% of that fitted in the range of 1.8–3.3 nm. The shapes of the larger particles were also not uniform and were observed as either aggregates and agglomerates.

$N_2$ -saturated aqueous solutions also showed similar sequences during sonication. However, the reaction proceeded slowly, requiring 50 min for completion. The UV-vis spectrum of the final solution was very similar to that obtained in the case of Ar. The electron micro-

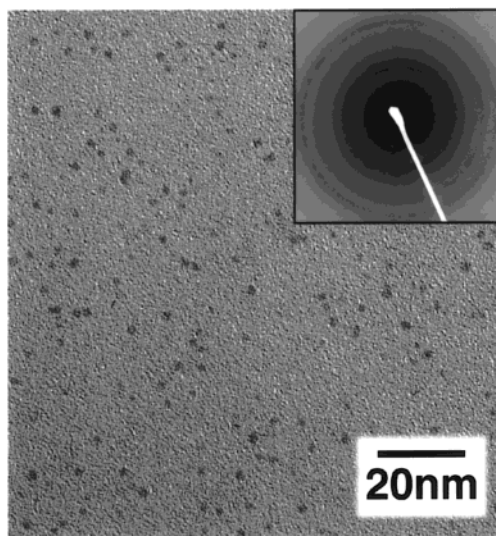


**Figure 2.** Electron micrograph and SAED pattern of Pd nanoparticles prepared under a  $N_2$  atmosphere.

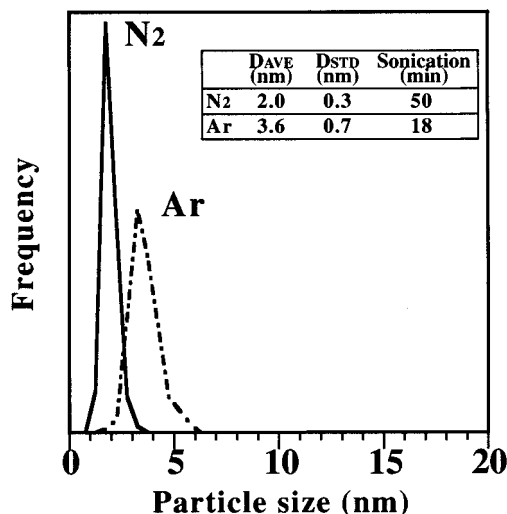


**Figure 3.** Particle size distributions of Pd nanoparticles prepared under  $N_2$  or Ar atmospheres.

graph of the Pd nanoparticles prepared under a  $N_2$  atmosphere is shown in Figure 2, together with the selected-area electron beam diffraction (SAED) pattern. Four Debye-Scherrer rings corresponding to the {111}, {200}, {220}, and {311} directions of a fcc lattice were observed in the SAED pattern. The particles were observed to have a spherical shape and a higher uniformity in both size and shape.  $D_{AVE}$  and  $D_{STD}$  were 2.0 and 0.3 nm, respectively. The size distributions of the Pd particles prepared under  $N_2$  and Ar are represented in Figure 3.

**3.2. Platinum Nanoparticles.** The clear yellow-colored aqueous  $H_2PtCl_6$  solution under an Ar atmosphere changed to very pale grayish-yellow and then turned dark brown upon ultrasonic irradiation. In the UV-vis spectrum, absorption bands at around 375 nm and below 300 nm first decayed (0–50 min), and after that, an increase of the baseline was observed during the sonication. Only a few Pt particles were observed in electron micrographs of the sample prepared from the solution after the first stage of sonication. The solution color became darker upon further sonication, and the reaction was completed in 120 min of sonication.

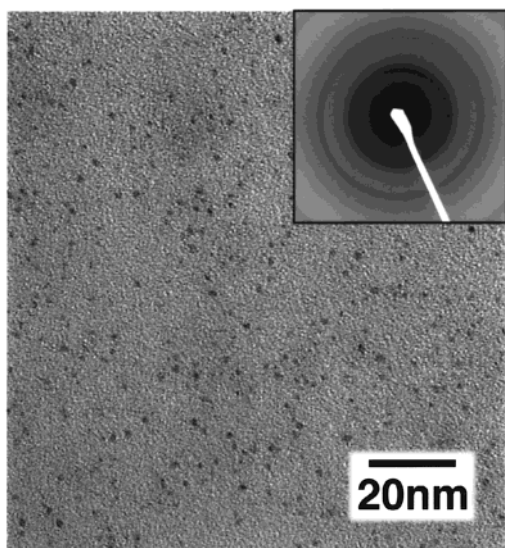


**Figure 4.** Electron micrograph and SAED pattern of Pt nanoparticles prepared under a Xe atmosphere.

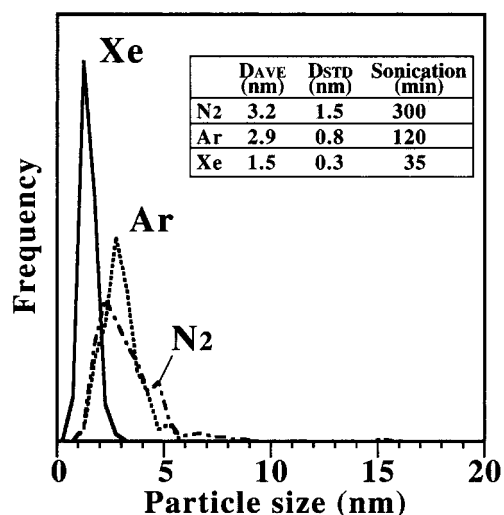


**Figure 5.** Particle size distributions of Pt nanoparticles prepared under N<sub>2</sub>, Ar, and Xe atmospheres.

In the electron micrographs, irregular particle shapes were found. Most particles were agglomerates that consisted of a few primary particles.

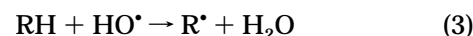
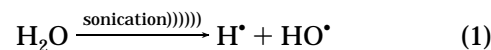
A similar reaction sequence was observed for the N<sub>2</sub>-saturated solution. However, the reaction rate was very low. The time required to complete the first stage was 140 min, and the reaction was finished after 300 min of sonication. The particles were irregular in both size and shape. Most particles were agglomerates.

Under Xe atmosphere, an acceleration of the reaction rate was also observed. The first stage of the reaction was completed within 8 min, and the reaction was finished after 35 min. Figure 4 shows an electron micrograph and the SAED pattern of the Pt nanoparticles prepared under a Xe atmosphere. In the SAED pattern, three Debye–Scherrer rings were observed. The diffraction pattern shows good agreement with the simulated diffraction profile of a fcc metal nanoparticle having a size of 1.6 nm.<sup>11</sup> Uniform particles, both in shape and size, are observed in the electron micrograph.

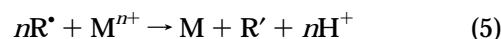
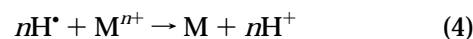
$D_{AVE}$  and  $D_{STD}$  are 1.5 and 0.3 nm, respectively. The size distributions of the Pt particles prepared under N<sub>2</sub>, Ar, and Xe are represented in Figure 5. In contrast with the case of Pd, a sharper size distribution was observed with Pt nanoparticles prepared under a Xe atmosphere.

#### 4. Discussion

Metal ions can be reduced by radicals produced by acoustic cavitation. The expected sequence of reactions that would lead to the formation of novel metal nanoparticles is shown in eqs 1–6.<sup>3,12</sup>



where RH denotes PVP or 2-propanol



where  $\text{R}' + \text{H} = \text{R}$



In the cases of both Pd and Pt, the reaction rates show the same tendency for the dissolved gases. The reaction rates are in the following order: under Xe > under Ar > under N<sub>2</sub>. This relationship can be interpreted by the hot-spot temperature produced by acoustic cavitation. The hot-spot temperature depends on the heat capacity ratio ( $\gamma = C_p/C_v$ ) and thermal conductivity of the gas inside the bubble.<sup>9,13</sup> Although the heat capacity ratios of Xe (1.66) and Ar (1.67) are almost the same, the thermal conductivity of Xe is less than one-third that of Ar. Because the lower thermal conductivity of the dissolved gas produces a higher temperature during cavitation collapse, the rapid reaction rate under Xe can be explained by the higher hot-spot temperatures at which greater amounts of radicals are produced (eqs 1 and 2). In the case of N<sub>2</sub>, the higher thermal conductivity and smaller heat capacity ratio compared with those of Ar produce a lower hot-spot temperature, which causes a decreased reaction rate.

The average particle sizes for Pd and Pt inversely depend on the dissolved gases. The smallest Pd particles were formed with N<sub>2</sub>. By changing the gas to Ar or Xe, the sonication time became shorter, and the  $D_{AVE}$  values increased. On the other hand, the smallest Pt particles were formed with Xe. The sonication time became longer, and the  $D_{AVE}$  values increased when the gas was changed to Ar or N<sub>2</sub>. It is notable that the best monodispersivities were observed under the conditions at which the smallest particles were formed and similar sonication times had been applied. This result indicates that there is an optimum sonication time for the preparation of monodispersion nanoparticles. The sonication time of 50 min provides the best monodispersivity (Pd/N<sub>2</sub>), with a normalized standard deviation of 15%.

(12) Flint, E. B.; Suslick, K. *J. Phys. Chem.* **1991**, *95*, 1484.

(13) The hot-spot temperature is proportional to  $(\gamma - 1)$ . See Neppiras, E. A. *Phys. Rep.* **1980**, *61*, 159.

(11) Hall, B. D. *J. Appl. Phys.* **2000**, *87*, 1666.

The particle size uniformity decreases with higher reaction rates, and it also gradually decreases with lower reaction rates.

The particles are formed by the collision of reduced metal ions (eq 6) and stabilized by coexisting polymers. The particle growth process and the stabilization process can competitively occur through the quick supply of metal atoms, which causes the inhomogeneity of the particle size and shape (Pd/Xe, Pd/Ar). In the case of longer sonication times, collisions of the smaller nanoparticles could occur (Pt/Ar, Pt/N<sub>2</sub>). Doktycz and Suslick reported particle agglomerations in hydrocarbon solutions through interparticle collisions driven by ultrasound.<sup>14</sup> According to their estimation, localized effective temperatures at the point of impact for particles exceed 2873 K. The speed of sound in hydrocarbons is roughly 1100 m/s, whereas in water, it is roughly 1500 m/s. By definition, shock waves generated by cavitation will have velocities greater than the speed of sound. The shock wave pressures in aqueous solution will be greater than those in hydrocarbons, causing greater velocities

for the particles.<sup>15</sup> The localized effective temperatures at the point of impact for Pt nanoparticles will exceed 2873 K, which is enough to spot-weld the Pt particles together. The particle shapes for the longer sonication times (Pt/Ar, Pt/N<sub>2</sub>) were agglomerates, which is in accord with this suggestion.

### 5. Conclusion

Pd nanoparticles having a sharp size distribution were prepared by sonication of an aqueous Pd salt solution under a N<sub>2</sub> atmosphere. In the case of Pt, a sharper size distribution was achieved under a Xe atmosphere. In both cases, similar sonication times were applied. Results suggest that there is an optimum sonication time for preparing single-dispersion nanoparticles using ultrasound. Consequently, it is important that the reaction rates be controlled. Because the reaction rate depends on the hot-spot temperature, it can be controlled by changing the dissolved gas.

CM000910F

---

(14) Doktycz, S. J.; Suslick, K. *Science* **1990**, *247*, 1067.

(15) Cole, R. H. *Underwater Explosions*; Princeton University Press: Princeton, NJ, 1948.